NATIONAL ADVISORY COMMITTEE FOR AERONAUTICS

TECHNICAL NOTE 3429

STATIC STABILITY OF FUSELAGES HAVING A RELATIVELY FLAT CROSS SECTION

By William R. Bates

Langley Aeronautical Laboratory
Langley Field, Va.

Washington
March 1955

NATIONAL ADVISORY COMMITTEE FOR AERONAUTICS

TECHNICAL NOTE 3429

STATIC STABILITY OF FUSELAGES HAVING A RELATIVELY FLAT CROSS SECTION[1]

By William R. Bates

SUMMARY

An investigation has been conducted in the Langley free-flight tunnel to determine the static stability characteristics of several fuselages having a relatively flat cross section and a high fineness ratio.

The results showed that, at high angles of attack for flat fuselages with the major cross-sectional axis horizontal, the flat nose caused a strong sidewash which caused these fuselages to be directionally stable for the center of gravity considered, which was two-thirds the fuselage length behind the nose. This sidewash also caused a vertical tail on these fuselages to be directionally destabilizing at small angles of sideslip.

INTRODUCTION

Recently some proposed airplane designs have incorporated fuselages having a relatively flat cross section with the major cross-sectional axis horizontal. Information on which to base estimates of the directional stability of such fuselages was not available. It seemed that the flat nose section of the fuselage might cause the same type of flow as that caused by the horizontal tail of a canard model previously tested by the NACA (reference 1). The combination of the fuselage and horizontal tail of this canard model was directionally unstable at low angles of attack, but at high angles of attack the sidewash from the horizontal tail caused an effective reversal in the direction of sideslip of the fuselage so that the combination was directionally stable. Since it was believed that the directional stability of the flat fuselage might vary considerably with angle of attack, as was the case with the canard model, an investigation was made in the Langley free-flight tunnel to determine the static stability characteristics of several fuselage models having a relatively flat cross section. This

---

[1]Supersedes recently declassified NACA RM L9I06a, 1949.

investigation also included a determination of the effect of a canopy and of several vertical and horizontal surfaces.

SYMBOLS

All forces and moments are referred to the stability axes which are defined in figure 1. The symbols and coefficients used in the present paper are:

S	wing area, square feet
$\bar{c}$	wing mean aerodynamic chord, feet
b	wing span, feet
A	aspect ratio (b^2/S)
q	dynamic pressure, pounds per square foot $\left(\frac{1}{2}\rho V^2\right)$
V	airspeed, feet per second
ρ	air density, slugs per cubic foot
α	angle of attack of fuselage chord line, degrees
δ_N	deflection of forward third of the fuselage (positive for nose-up deflection), degrees
β	angle of sideslip, degrees
ψ	angle of yaw, degrees
i_t	angle of incidence of the horizontal tail, degrees
C_L	lift coefficient (Lift/qS)
C_D	drag coefficient (Drag/qS)
C_m	pitching-moment coefficient (Pitching moment/qS$\bar{c}$)
C_n	yawing-moment coefficient (Yawing moment/qSb)
C_l	rolling-moment coefficient (Rolling moment/qSb)

C_Y lateral-force coefficient (Lateral force/qS)

C_{L_α} rate of change of lift coefficient with angle of attack per degree $(\partial C_L/\partial\alpha)$

C_{n_β} rate of change of yawing-moment coefficient with angle of sideslip per degree $(\partial C_n/\partial\beta)$

C_{l_β} rate of change of rolling-moment coefficient with angle of sideslip per degree $(\partial C_l/\partial\beta)$

C_{Y_β} rate of change of lateral-force coefficient with angle of sideslip per degree $(\partial C_Y/\partial\beta)$

APPARATUS AND TESTS

Sketches of the models used in the investigation are presented in figure 2. The geometric characteristics of the models are presented in table I. For convenience in discussion, the models will be referred to by the number designation shown in this table. Model 5 was slightly larger than models 1 to 3, and the force and moment coefficients for this model were therefore corrected by multiplying the measured values by the ratio of the volume of model 1 to the volume of model 5 so that they would be directly comparable with those of models 1 to 3. The sketch shown in figure 2 shows model 5 reduced to the same volume as model 1.

Force tests to determine the aerodynamic characteristics of the models were made on the six-component balance in the Langley free-flight tunnel. These facilities are described in references 2 and 3. All the force tests were made at a dynamic pressure of 4.093 pounds per square foot which corresponds to a Reynolds number of approximately 318,500 based on the mean aerodynamic chord of the assumed wing.

Tests were made to determine the static longitudinal stability characteristics of the fuselages alone and also with various fin configurations. (See fig. 3.) The lateral stability characteristics of the fuselages alone and with a horizontal tail and various vertical surfaces added were determined in two ways. A general impression of the variation of the lateral stability characteristics with angle of attack was obtained by determining the static lateral-stability derivatives from the difference between the measurements of the force and moment coefficients in tests at 5° and -5° yaw. In order to determine how well these stability

derivatives represented the variation of the lateral-stability coefficients with angle of yaw, the lateral-stability coefficients were determined from tests over a range of yaw angle from 20° to -20° for three angles of attack. A survey of the flow around model 1 was made with streamers of string attached to the fuselage.

RESULTS AND DISCUSSION

The presentation of the test results and the analysis of the data have been grouped into two main sections. The first section deals with the static lateral and longitudinal stability characteristics of the fuselages alone for which the flow survey and force-test data are presented in figures 4 to 8. The second section deals with the effect of the canopy and the various horizontal and vertical tails and control surfaces on the static lateral and longitudinal stability and control characteristics of the models. The force-test data for these configurations are presented in figures 9 to 16. The force and moment coefficients of all the models were based on the dimensions of an arbitrarily chosen wing which is shown in dashed lines in figure 2. All the moment data are referred to a point two-thirds the fuselage length behind the nose of the fuselage. This point was chosen to represent the center-of-gravity position for a tailless airplane having a fuselage such as those tested. This center of gravity does not correspond to the center of gravity of a conventional airplane; therefore the data could not be used directly for a conventional airplane configuration.

Fuselages Alone

Lateral stability.— The results of force tests made to determine the lateral stability characteristics of the fuselages alone are presented in figures 5 to 7. These data show that at 0° angle of attack all of the fuselages were unstable, as would be expected. As the angle of attack was increased, the models which have their major cross-sectional axis horizontal (models 1, 3, and 4) became increasingly stable directionally, and at high angles of attack they became very stable. The reason for this increase in directional stability with increase in angle of attack is the unusual trend in side force. The results of the flow survey are presented in figure 4. These data show that the flow around the model was normal at low angles of attack but that there was a pronounced sidewash from the forward part of the fuselage which produced an effective reversal of the direction of sideslip of most of the fuselage at high angles of attack. This sidewash is similar to that obtained with the canard model of reference 1 where it was found that the horizontal tail caused a strong sidewash over the fuselage which effectively reversed the direction of sideslip of most of the fuselage. Observation

of the tufts on the top of the model in the present investigation indicated that there was a reversal in the flow, while the tufts on the bottom of the model lined up with the free-stream flow.

When the major cross-sectional axis of the flat fuselage was vertical (model 2), the model became increasingly unstable as the angle of attack was increased. Figures 5 and 6 also show that the lateral-force coefficient became greater as the angle of attack was increased. This increase in the lateral-force parameter $-C_{Y_\beta}$ with increasing angle of attack evidently results from the fact that the fuselage acts as a yawed wing where 0° angle of attack of the fuselage corresponds to 90° yaw of a wing and increasing angle of attack corresponds to reducing the angle of yaw of a wing. Increasing the angle of attack of the fuselage therefore results in an increase in $-C_{Y_\beta}$ just as reducing the angle of yaw of a wing results in an increase in C_{L_α}. Since the assumed center of gravity of this model is two-thirds the fuselage length behind the nose, it is behind the center of pressure, and the increase in $-C_{Y_\beta}$ with an increase in angle of attack therefore results in a decrease in C_{n_β} as the angle of attack is increased.

As shown in figures 5 and 6, the effective dihedral of the flat fuselages is negative at high angles of attack when the major cross-sectional axis is horizontal (models 1, 3, and 4) and is positive at high angles of attack when the major cross-sectional axis is vertical (model 2). This difference in sign of the dihedral effect evidently results from the difference in sign of the lateral-force characteristics of the models. Since the center of pressure is forward of the center of gravity, it is also above the center of gravity at positive angles of attack, so that the lateral force has a pronounced effect on the effective dihedral of the fuselages at high angles of attack.

Since the inverse camber made model 3 directionally stable at a lower angle of attack than model 1 (as shown in figure 5), the nose of model 3 was then deflected upward to determine whether the model could be made more directionally stable at 0° angle of attack. The data presented in figure 7 show that, when the forward 30 percent of the fuselage was deflected upward so as to increase the negative camber, the directional instability of model 3 was somewhat reduced at 0° angle of attack. These data indicate, however, that the fuselage cannot be made directionally stable at 0° angle of attack by increasing the negative camber a reasonable amount.

Longitudinal stability.– The results of the force tests made to determine the longitudinal stability characteristics of the fuselages alone are presented in figure 8. The data of this figure show that the lift and drag of models 1, 3, and 4 are much higher than those of model 2 at high angles of attack. The higher drag results partly from the fact that the flat fuselages with the major cross-sectional axis horizontal produce lift as low-aspect-ratio wings ($A \approx 0.2$) and consequently develop high induced drag. The data of figure 8 also show that the static longitudinal instability (as indicated by the slope of the pitching-moment curve) increases with increase in angle of attack when the major cross-sectional axis is horizontal (fuselages 1, 3, and 4); whereas there is essentially no change in static longitudinal stability with angle of attack when the major cross-sectional axis is vertical (fuselage 2). This increase in longitudinal instability with increase in angle of attack for models 1, 3, and 4 results from the increase in slope of the lift and drag curves with increase in angle of attack. The assumed center of gravity of these models is well behind the center of pressure so that the lift and drag have a pronounced effect on the pitching moment.

Fuselages With Various Vertical and Horizontal Surfaces

Lateral stability and control.– The results of the force tests made to determine the lateral stability and control characteristics of the models with various vertical surfaces are presented in figures 9 to 11.

The effectiveness of a normal vertical tail on models 1 and 2 is shown in figure 9 by the increments of the lateral-stability coefficients contributed by the vertical tail over a range of angles of yaw from 20° to -20°. These data show that on model 1 the vertical tail gave directionally destabilizing moments at small angles of yaw where the vertical tail was in the sidewash field produced by the flat nose of the fuselage but provided directionally stabilizing moments at high angles of yaw where the vertical tail was out of this sidewash field. On model 2, the vertical tail gave a stabilizing moment throughout the angle-of-yaw range as would be expected. The effect of dorsal and ventral fins on the lateral stability characteristics of model 4 are presented in figure 10. These fins had essentially no effect on the lateral stability characteristics at small angles of yaw (except at $\alpha = 32^\circ$). This result is similar to the effect of low-aspect-ratio dorsal fins on conventional fuselages. Figure 11 shows the effect of canopy location on the static lateral-stability derivatives of model 4. The canopy had very little effect on the characteristics of the model when the canopy was mounted in the rear position (1.61 ft behind the nose of the model) except that the directional stability and negative dihedral effect were slightly higher at the high angles of attack. However, with the canopy in the forward position (0.34 ft behind the nose of the model) the directional

stability of the model was considerably lower than that of the fuselage alone. This result indicates that, when located in the forward position, the canopy interfered with the flow over the nose of the model and thereby reduced the sidewash induced by the nose and decreased the directional stability of the model.

The data presented in figures 12 and 13 show the effect of the all-movable horizontal tail at the nose on the lateral stability characteristics of models 1 and 2. This tail was set at an angle of incidence of 15° relative to the fuselage center line. Previous NACA tests have shown that a horizontal tail of this type produces a strong sidewash in a manner similar to that of the flat nose of models 1, 3, and 4. This sidewash from the horizontal tail caused the directional stability of model 2 to increase with increasing angle of attack in a manner similar to that shown for the fuselage alone on models 1, 3, and 4. This horizontal tail had no appreciable effect on the directional stability at 0° angle of attack. The data of figure 12 also indicate that the sidewash from the horizontal tail reinforced that from the nose of model 1 so that the directional stability of the model was greater with than without the horizontal tail at high angles of attack. The horizontal tail also caused model 1 to be stable at low angles of attack. Evidently the horizontal tail produced a sidewash over the fuselage at low angles of attack which effectively reversed the direction of sideslip of the fuselage so that the normally unstable moment of the fuselage was directionally stabilizing in this case.

The effect of asymmetric horizontal fins 3 and 4 (model 1) in producing moments for lateral control is shown in figure 14. These data show that fins 3 and 4 at the nose of the model produce rolling and yawing moments and lateral forces which increase as the angle of attack increases. The magnitude of these moments and forces varies almost directly with the size of the fin. Fin 5, which was mounted at the rear of the fuselage not as a lateral control but to balance partially the pitching moment of the forward fin, had essentially no effect on the lateral forces and moments.

Longitudinal stability.— The results of the force tests made to determine the longitudinal stability characteristics of models 1 and 4 with various horizontal fins are presented in figures 15 and 16, respectively. As shown in figure 15, the asymmetric fins forward of the center of gravity (fins 3 and 4), which were intended primarily as a lateral-control device, caused an increase in the nose-up pitching moment of the model. As would be expected, the fin behind the center of gravity (fin 5) caused the nose-up pitching moment of model 1 with fin 4 to become less. The pitching moment caused by the forward fins (3 and 4) is approximately proportional to the product of the fin area and moment arm. Based on the product of its area and moment arm, however, the rear fin is much less effective than the front fins, probably because of the downwash from the fuselage over the rear fin. Figure 16 shows that

the low-aspect-ratio fins (fin 6) on the rear of model 4 cause the static longitudinal instability of the model to become less.

CONCLUSIONS

An investigation conducted at the Langley free-flight tunnel to determine the static stability characteristics of several fuselages having a relatively flat cross section and a high fineness ratio led to the following conclusions:

1. At high angles of attack for the flat fuselages with the major cross-sectional axis horizontal, the flat nose caused a strong sidewash which caused these fuselages to be directionally stable for the center of gravity considered, which was two-thirds the fuselage length behind the nose.

2. The sidewash also caused a vertical tail on these fuselages to be directionally destabilizing at small angles of yaw.

3. A triangular-plan-form all-movable horizontal tail at 15° incidence caused the same type of sidewash effect as the flat nose of the fuselage with the major cross-sectional axis horizontal. When the major axis of the fuselage was horizontal, the sidewash from the horizontal tail reinforced that from the nose of the fuselage so that the directional stability of the fuselage was greater with than without the horizontal tail. When the major cross-sectional axis of the fuselage was vertical, the sidewash from the horizontal tail caused the directional stability of the model to increase with increasing angle of attack so that it was stable at high angles of attack.

Langley Aeronautical Laboratory,
National Advisory Committee for Aeronautics,
Langley Field, Va., December 9, 1949.

REFERENCES

1. Bates, William R.: Low-Speed Static Lateral Stability Characteristics of a Canard Model Having a 60° Triangular Wing and Horizontal Tail. NACA RM L9J12, 1949.

2. Shortal, Joseph A., and Osterhout, Clayton J.: Preliminary Stability and Control Tests in the NACA Free-Flight Wind Tunnel and Correlation With Full-Scale Flight Tests. NACA TN 810, 1941.

3. Shortal, Joseph A., and Draper, John W.: Free-Flight-Tunnel Investigation of the Effect of the Fuselage Length and the Aspect Ratio and Size of the Vertical Tail on Lateral Stability and Control. NACA WR L-487, 1943. (Formerly NACA ARR 3D17.)

TABLE I

CHARACTERISTICS OF THE FUSELAGE MODELS TESTED IN THE LANGLEY FREE-FLIGHT TUNNEL

Fuselage	Cross section	Plan form	Side elevation	Length (ft)	Volume (cu ft)
1	Elliptical	NACA 0014	NACA 0007	4.0	0.271
2	Elliptical	NACA 0007	NACA 0014	4.0	.271
3	Elliptical	NACA 0014	NACA 4407 inverted	4.0	.271
4	Elliptical	(a)	(a)	4.0	.447
5	Circular	(b)	(b)	6.38	.732

[a]The forward 30 percent of the length of model 4 was the same as that of model 1 and the rearward 70 percent of the length was an elliptical cylinder having the same cross section as the 30-percent station of the fuselage.

[b]Model 5 was a circular-cross-section fuselage having a fineness ratio of 12.75 and the maximum diameter at about the 47-percent station.

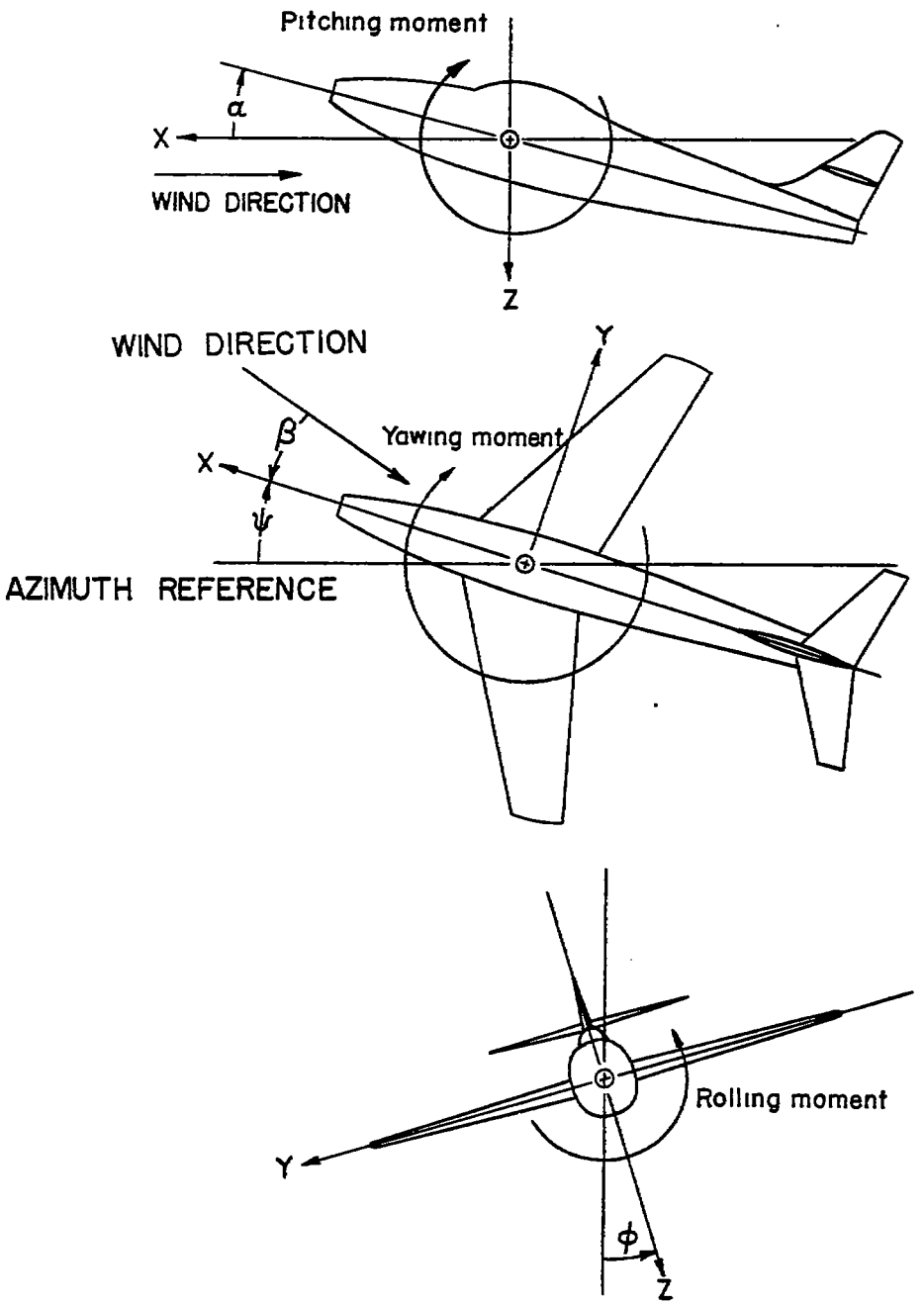

Figure 1.- The stability system of axes. Arrows indicate positive directions of moments, forces, and control-surface deflections. This system of axes is defined as an orthogonal system having the origin at the center of gravity and in which the Z-axis is in the plane of symmetry and perpendicular to the relative wind, the X-axis is in the plane of symmetry and perpendicular to the Z-axis, and the Y-axis is perpendicular to the plane of symmetry.

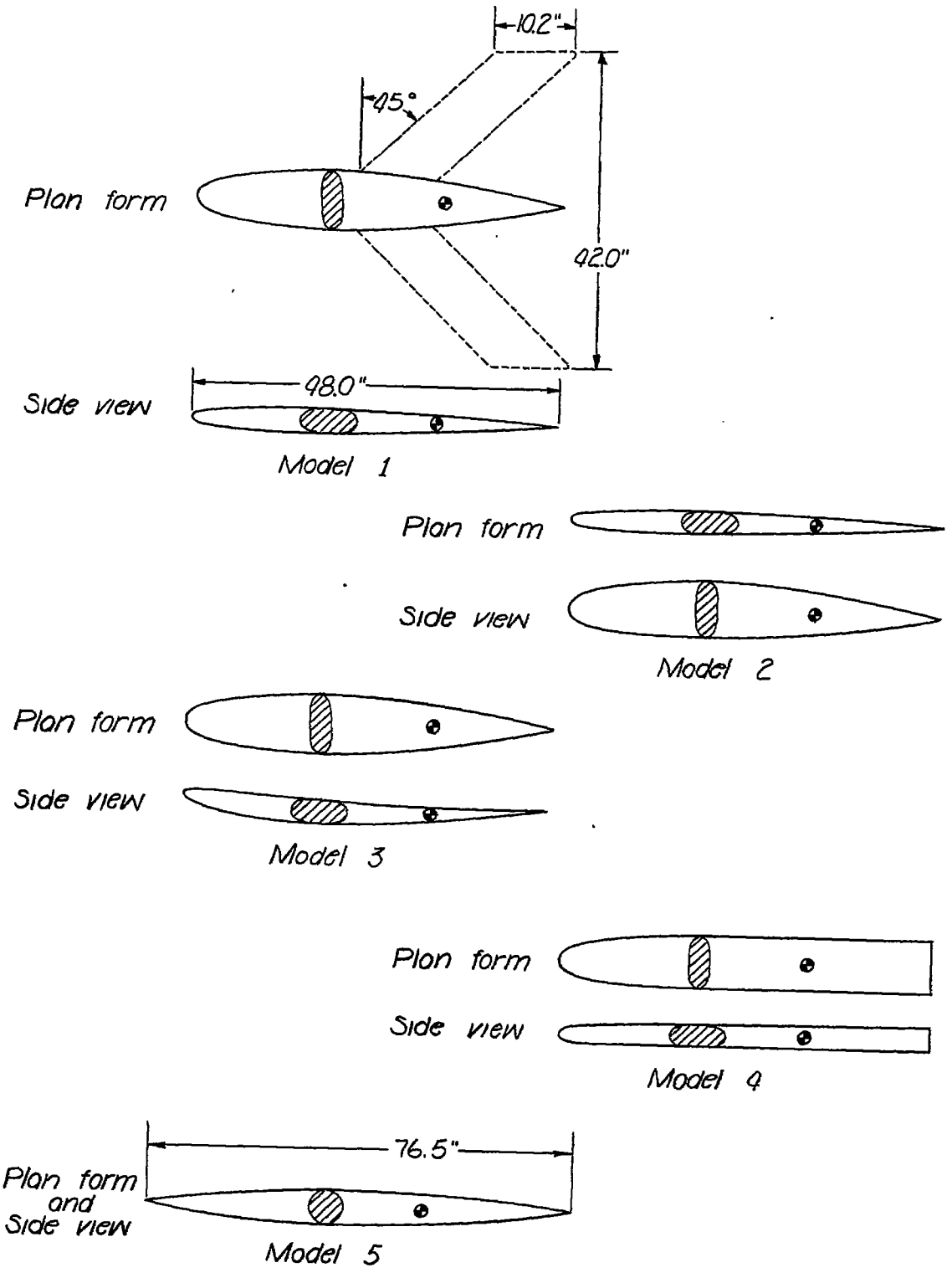

Figure 2.- Two-view drawings of the fuselage models.

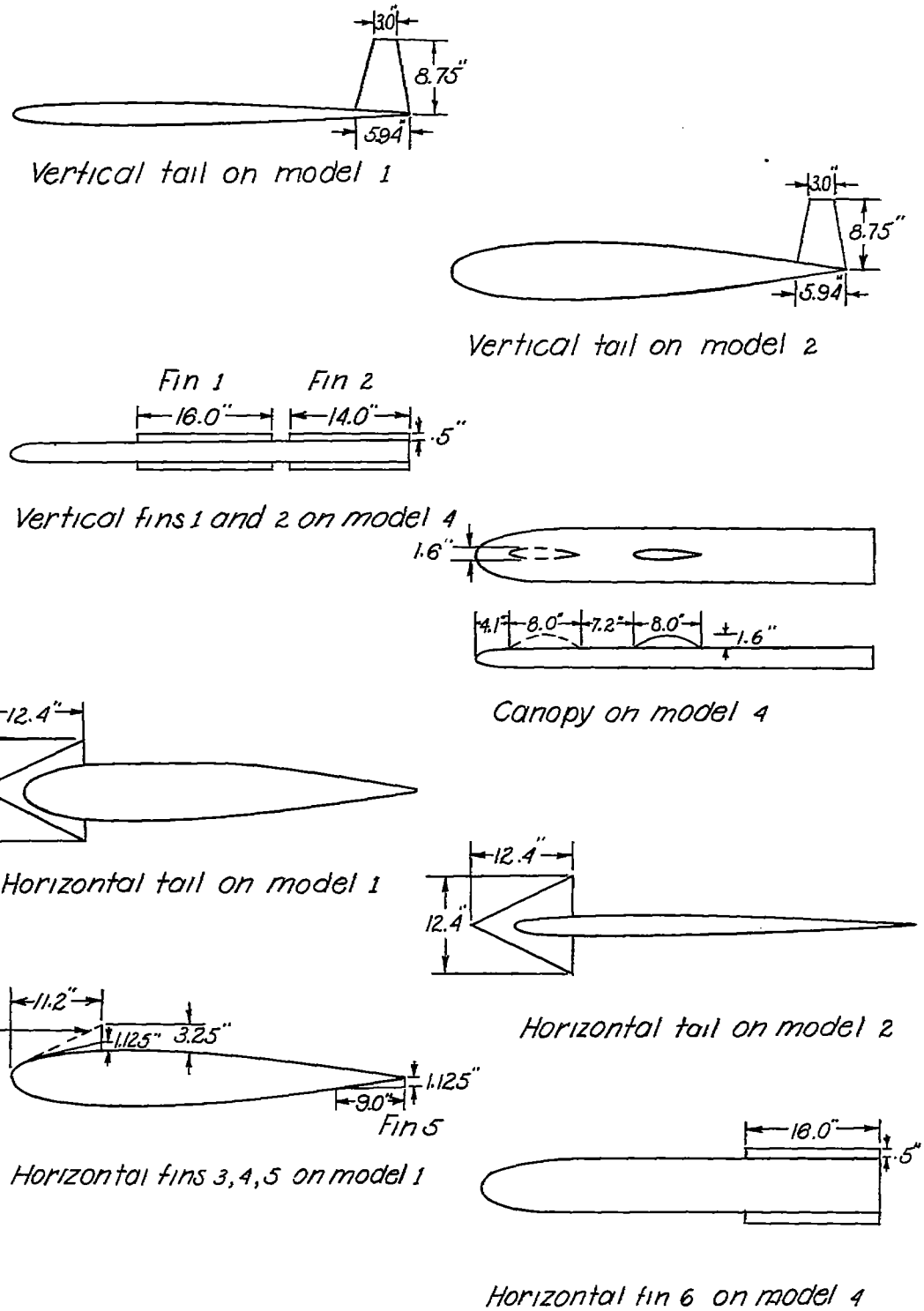

Figure 3.- Views of the fuselage models showing the vertical tail, vertical fins, canopy, horizontal tail, and horizontal fins.

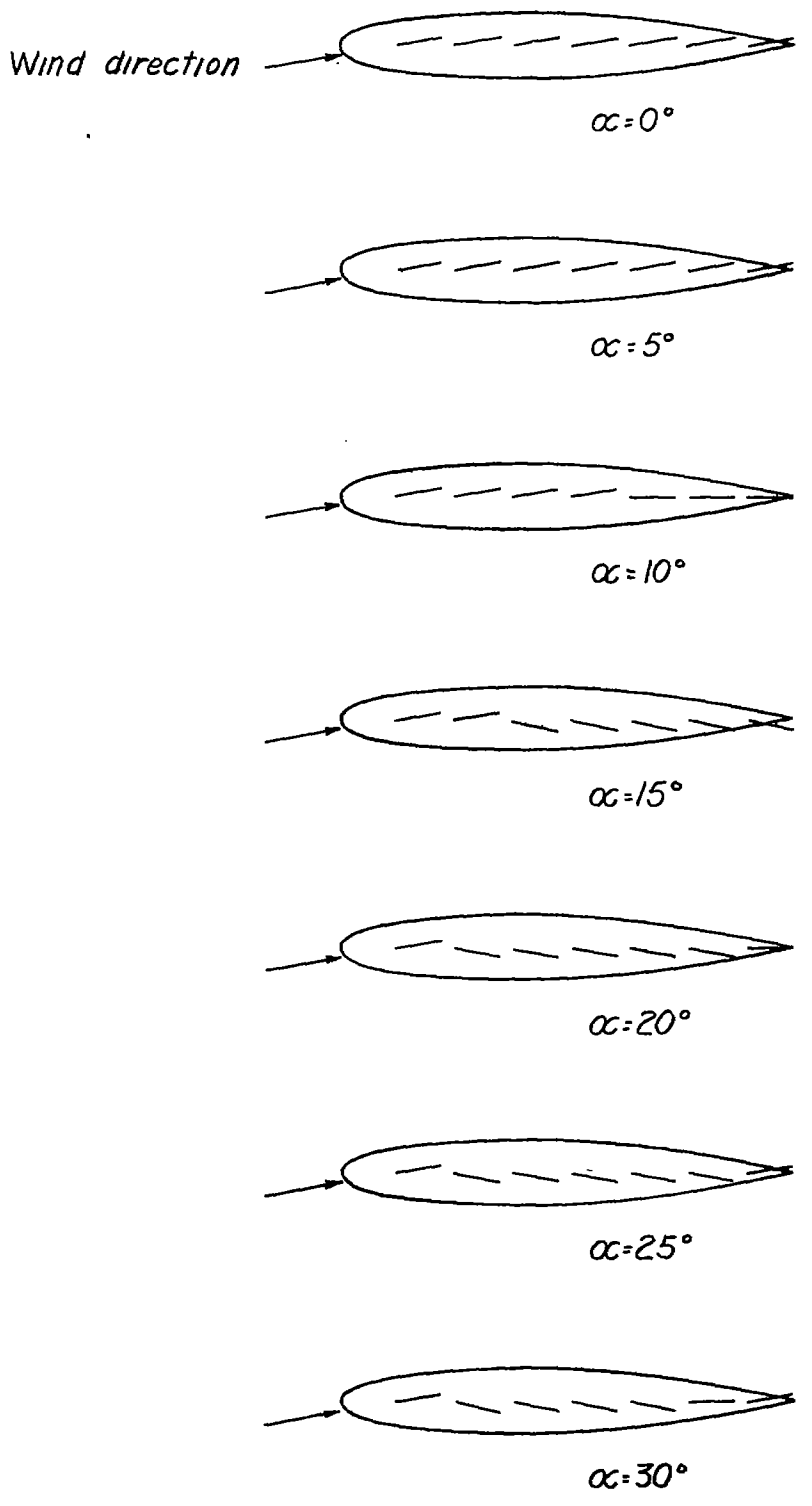

Figure 4.- Top of model 1 showing the flow at various angles of attack. $\psi = 5^{\circ}$.

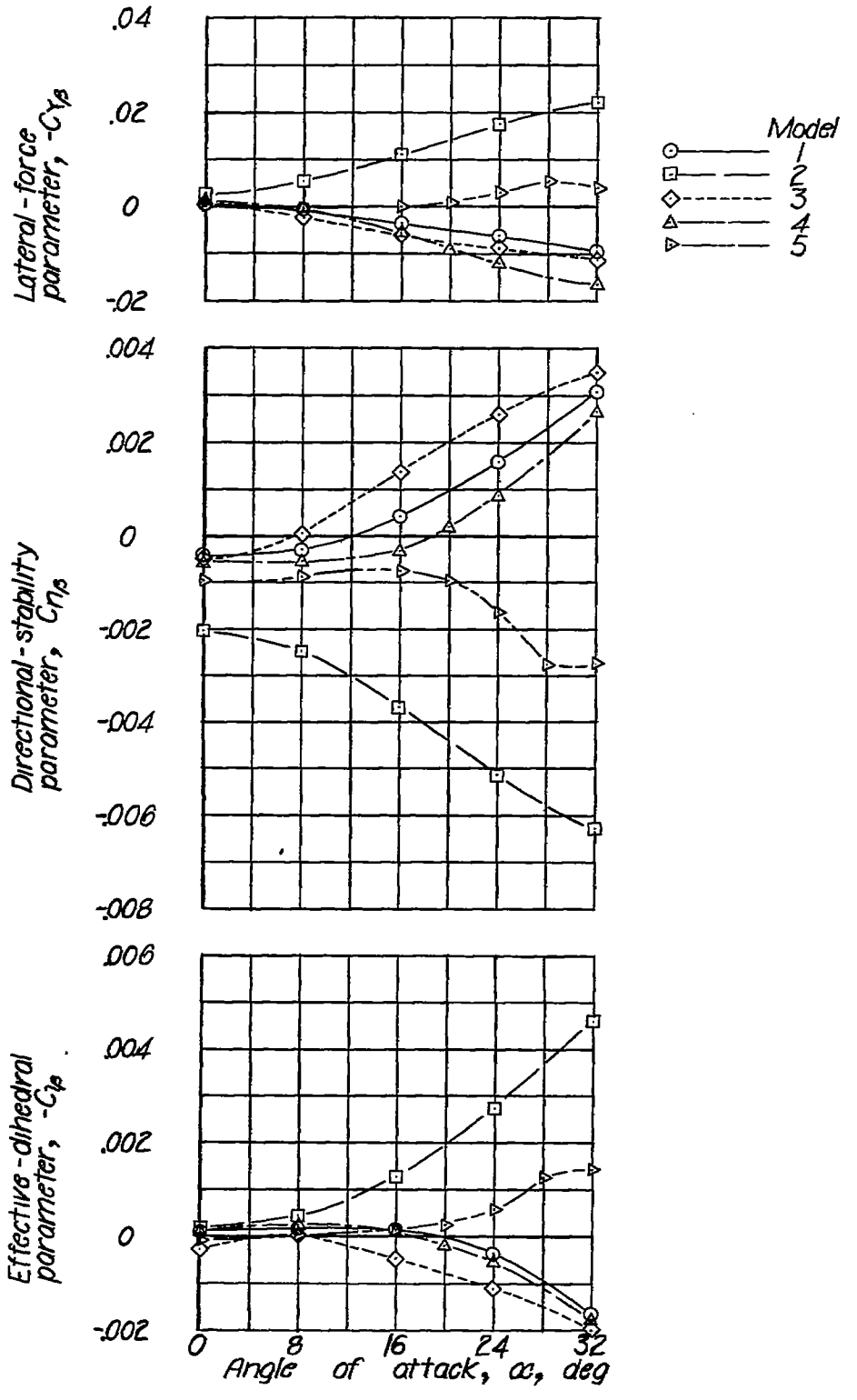

Figure 5.- Lateral stability characteristics of various fuselage models.

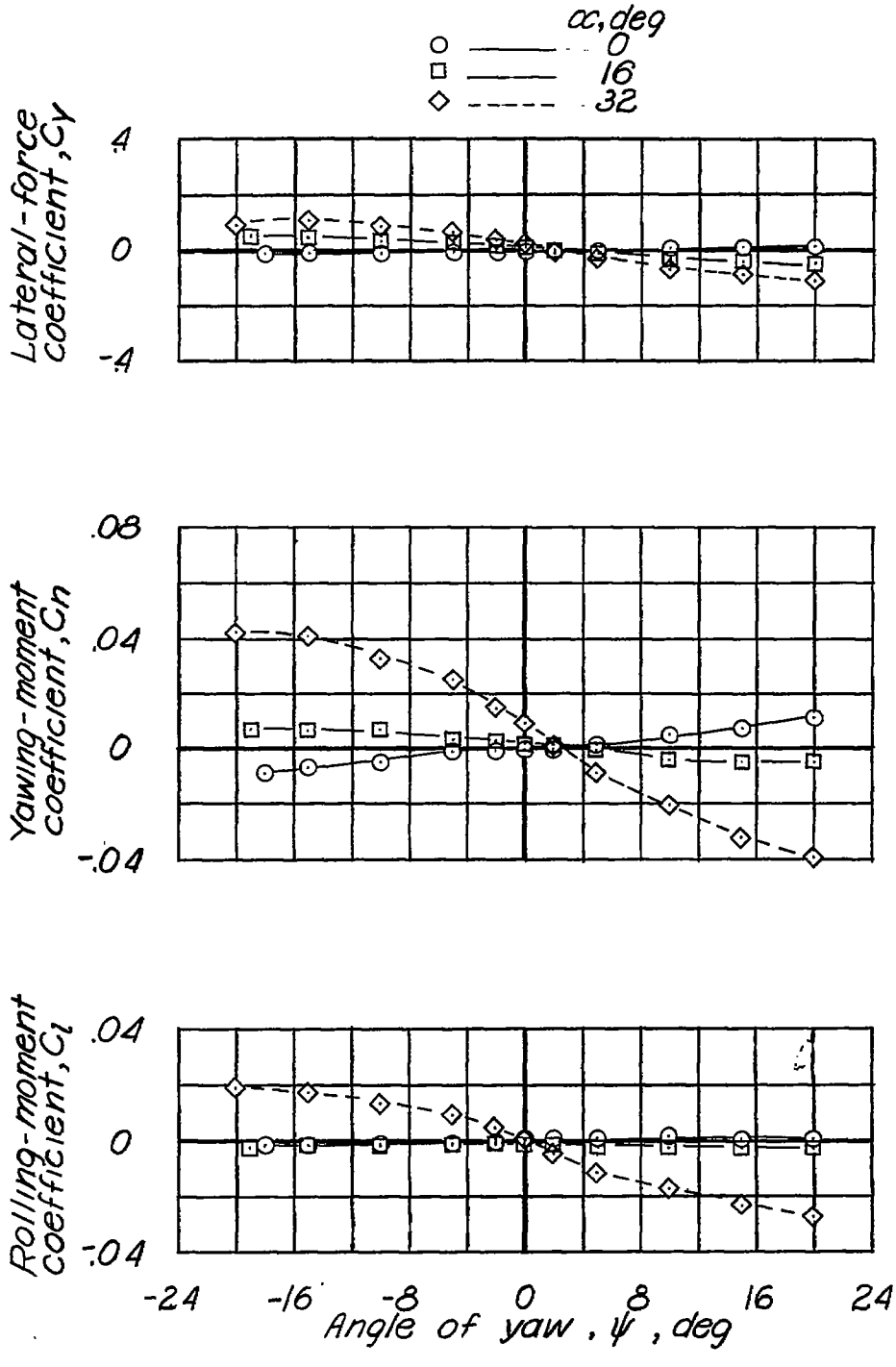

(a) Model 1.

Figure 6.- Effect of angle of attack on the lateral-stability coefficients of the fuselages alone.

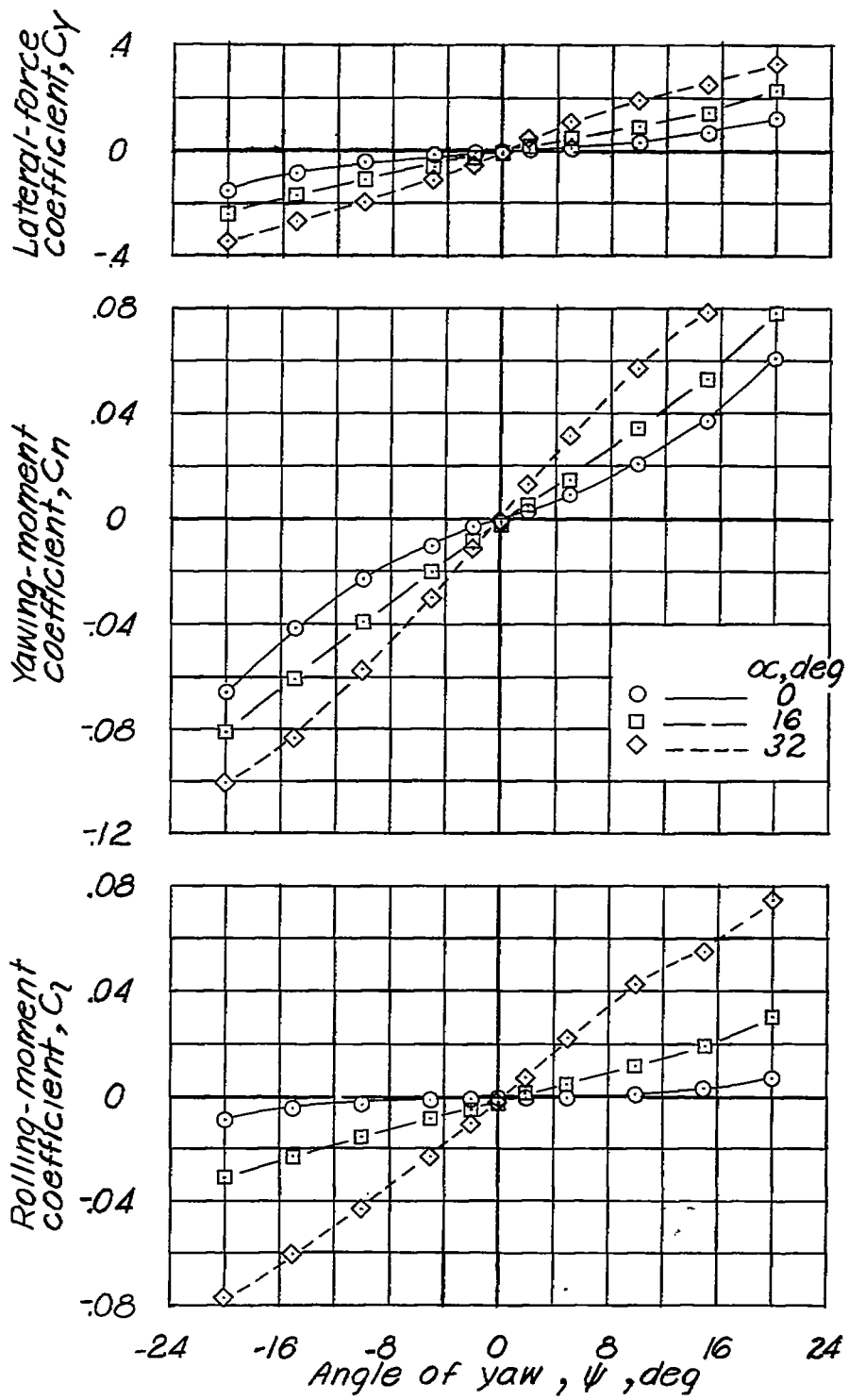

(b) Model 2.

Figure 6.- Continued.

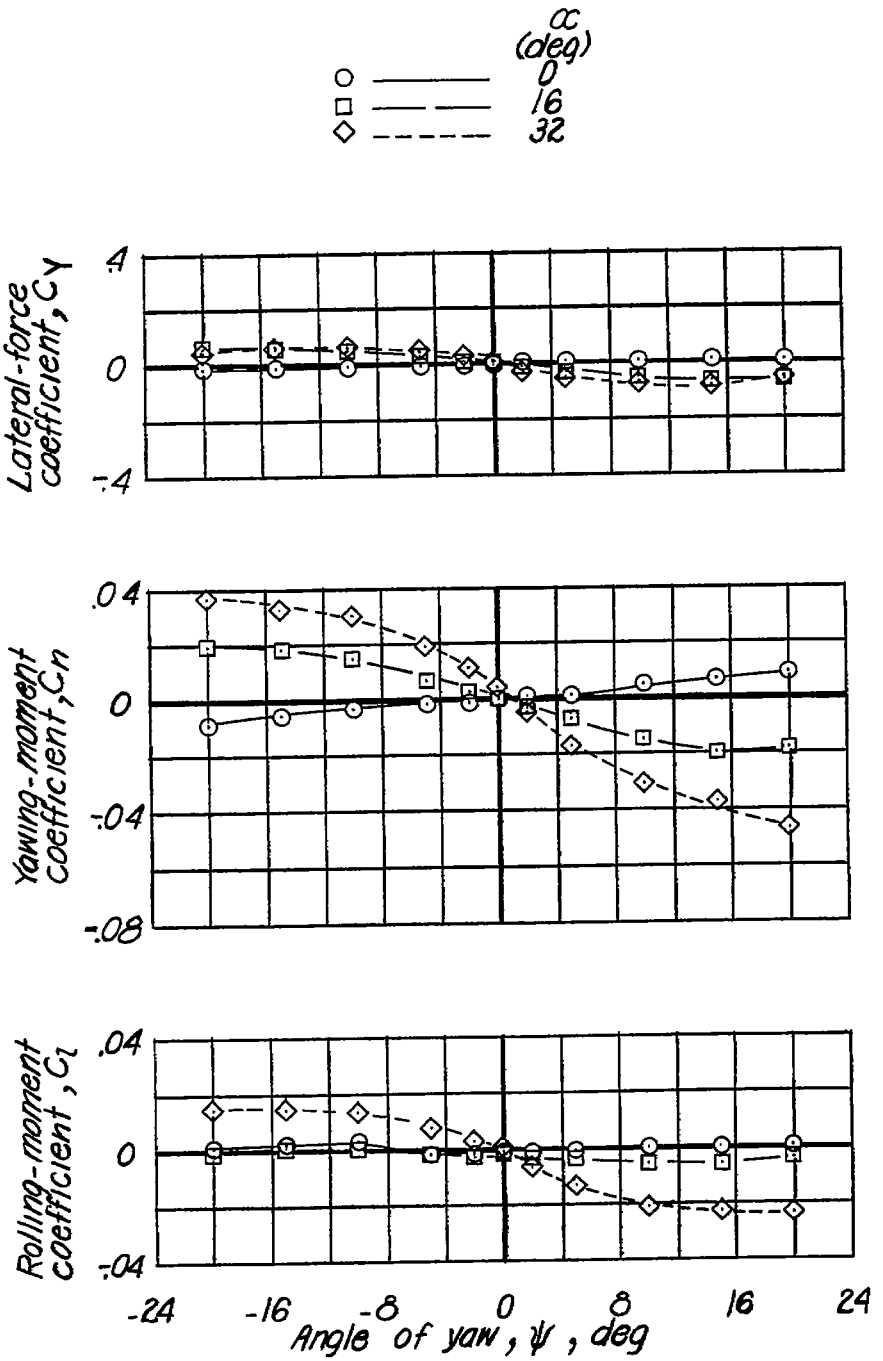

(c) Model 3.

Figure 6.- Continued.

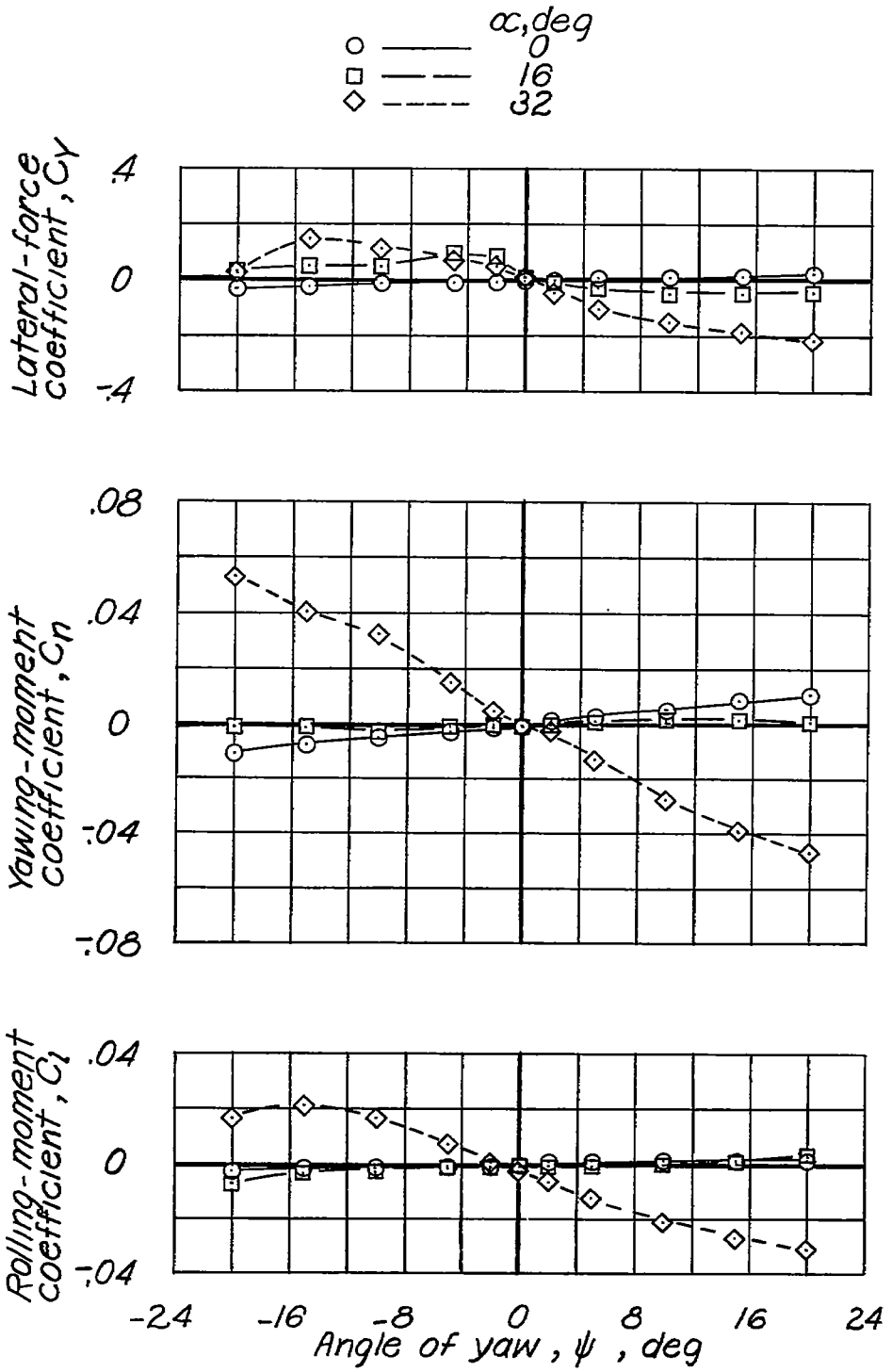

(d) Model 4.

Figure 6.- Concluded.

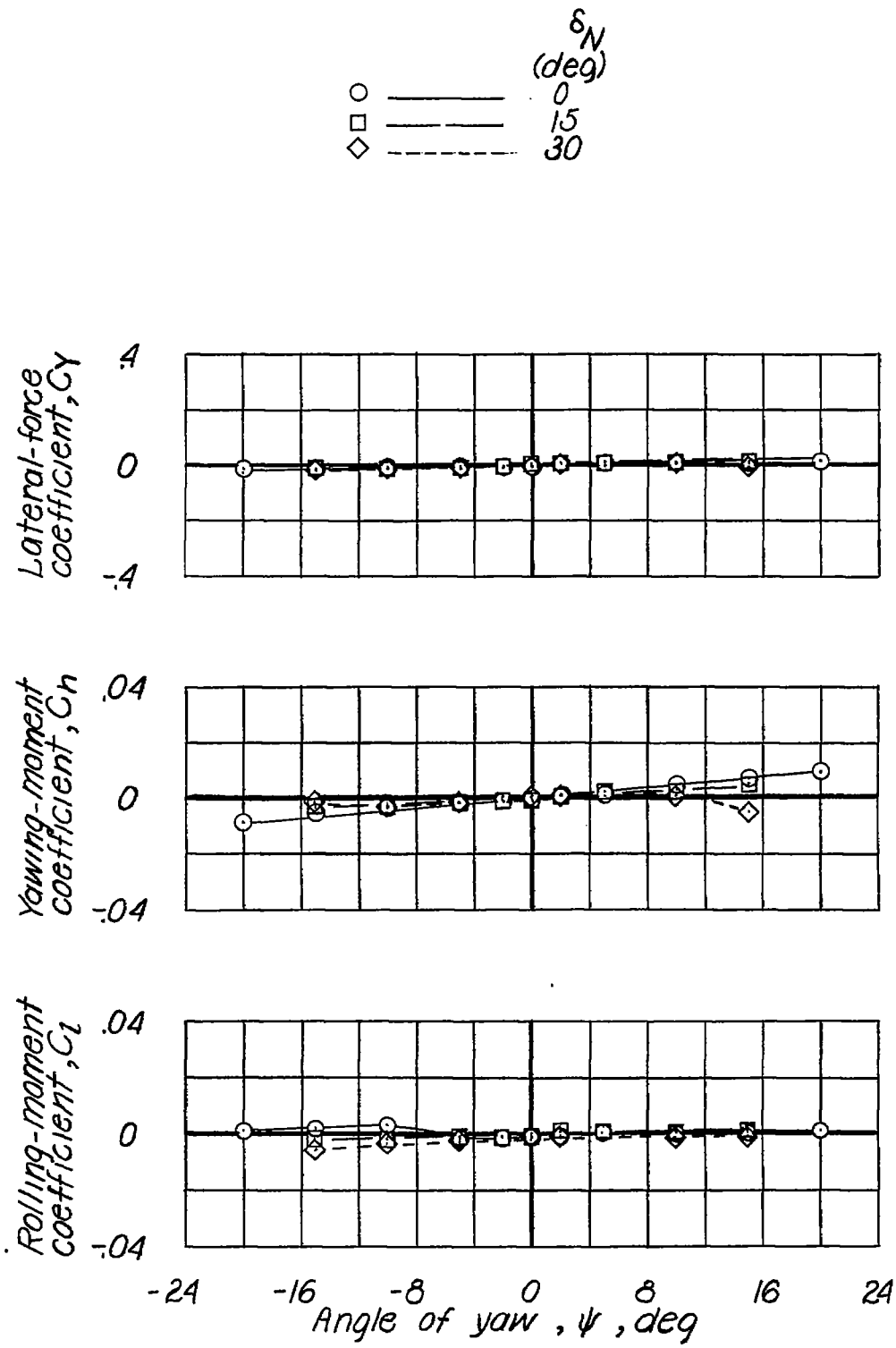

Figure 7.- Effect of deflecting the nose of model 3 on the lateral-stability coefficients. $\alpha = 0^\circ$.

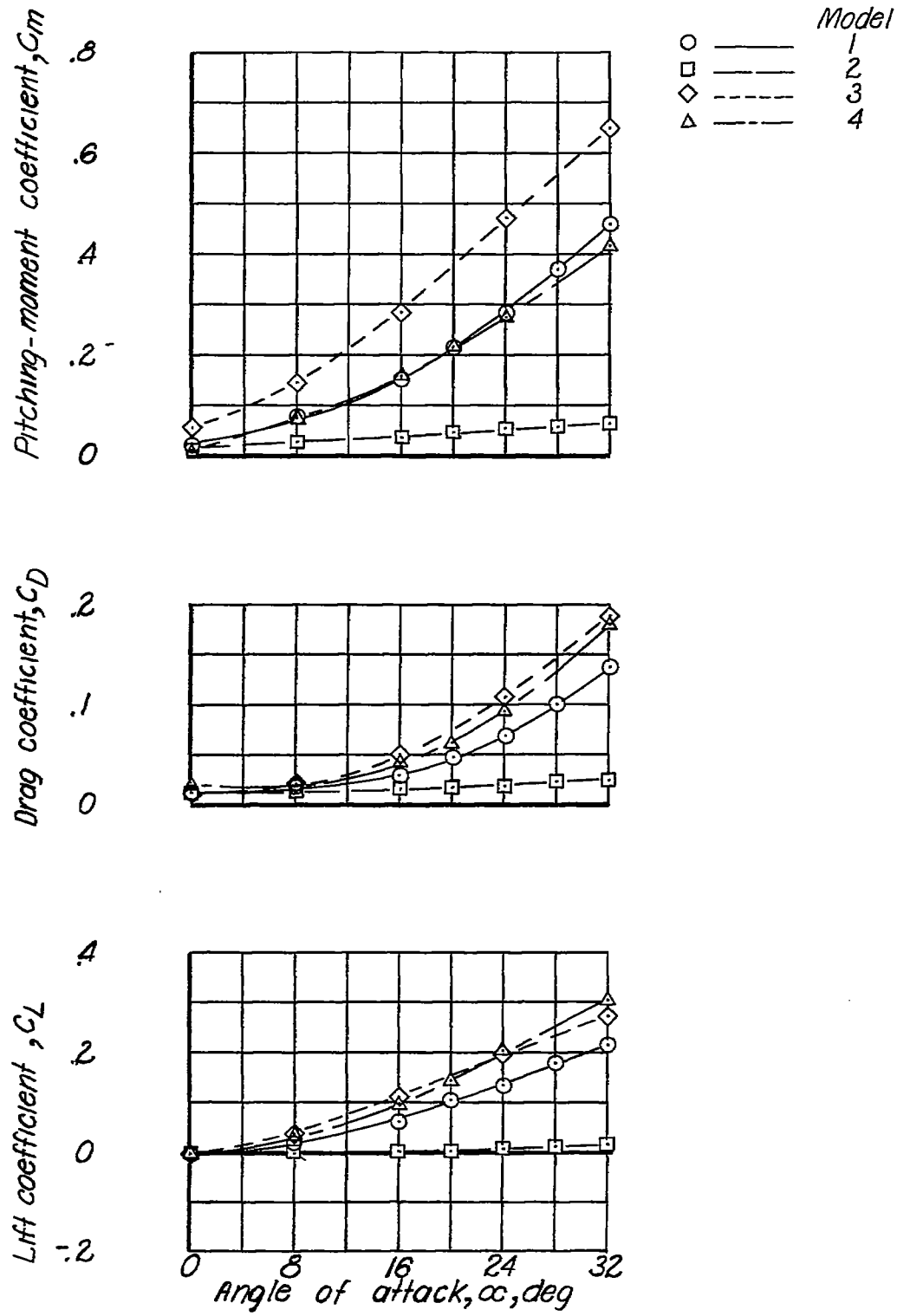

Figure 8.- Longitudinal stability characteristics of various fuselage models.

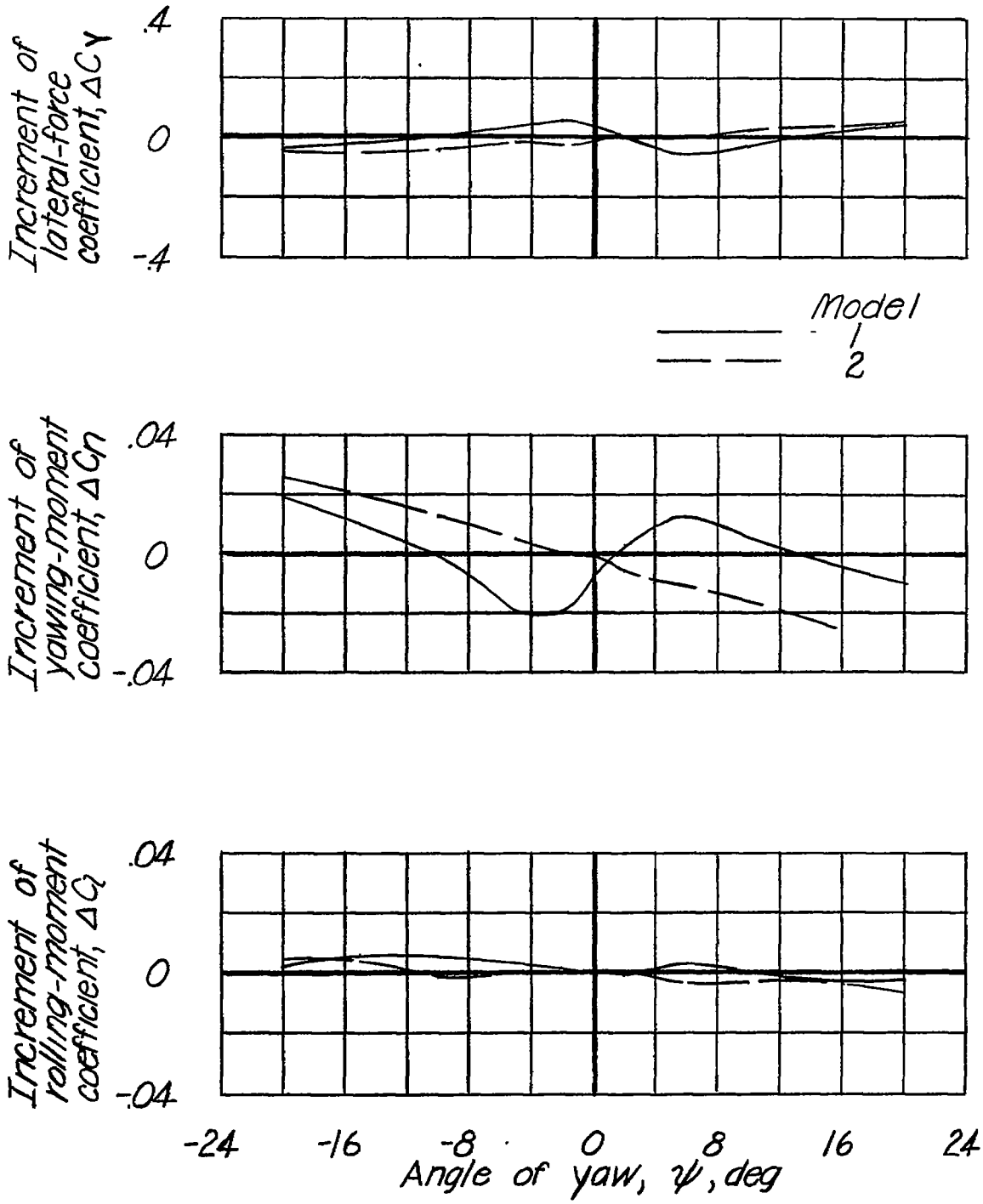

Figure 9.- Increments of lateral-stability coefficients caused by mounting a vertical tail on models 1 and 2. $\alpha = 32^{\circ}$.

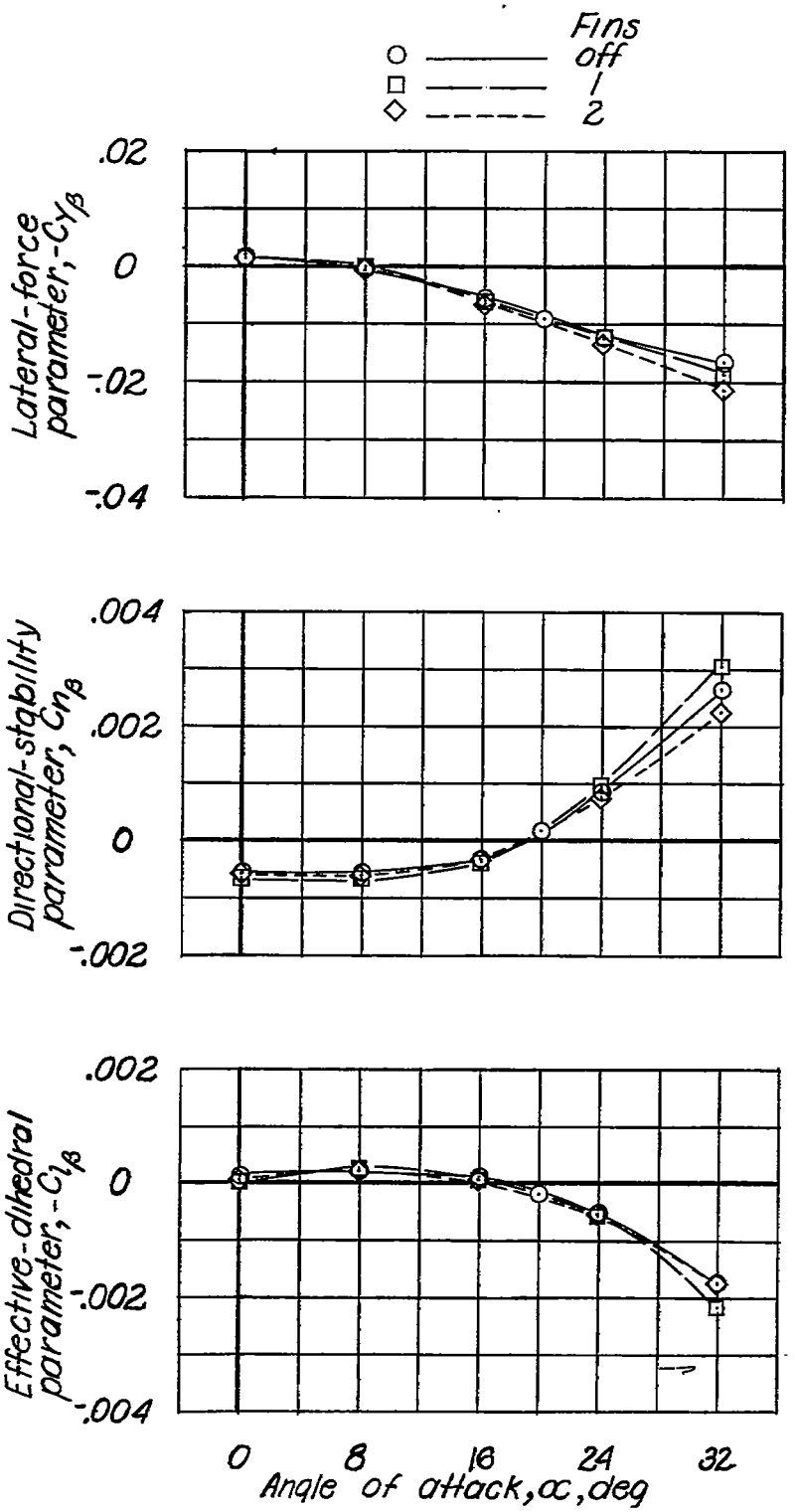

Figure 10.- Effect of dorsal and ventral fins on the lateral stability characteristics of model 4.

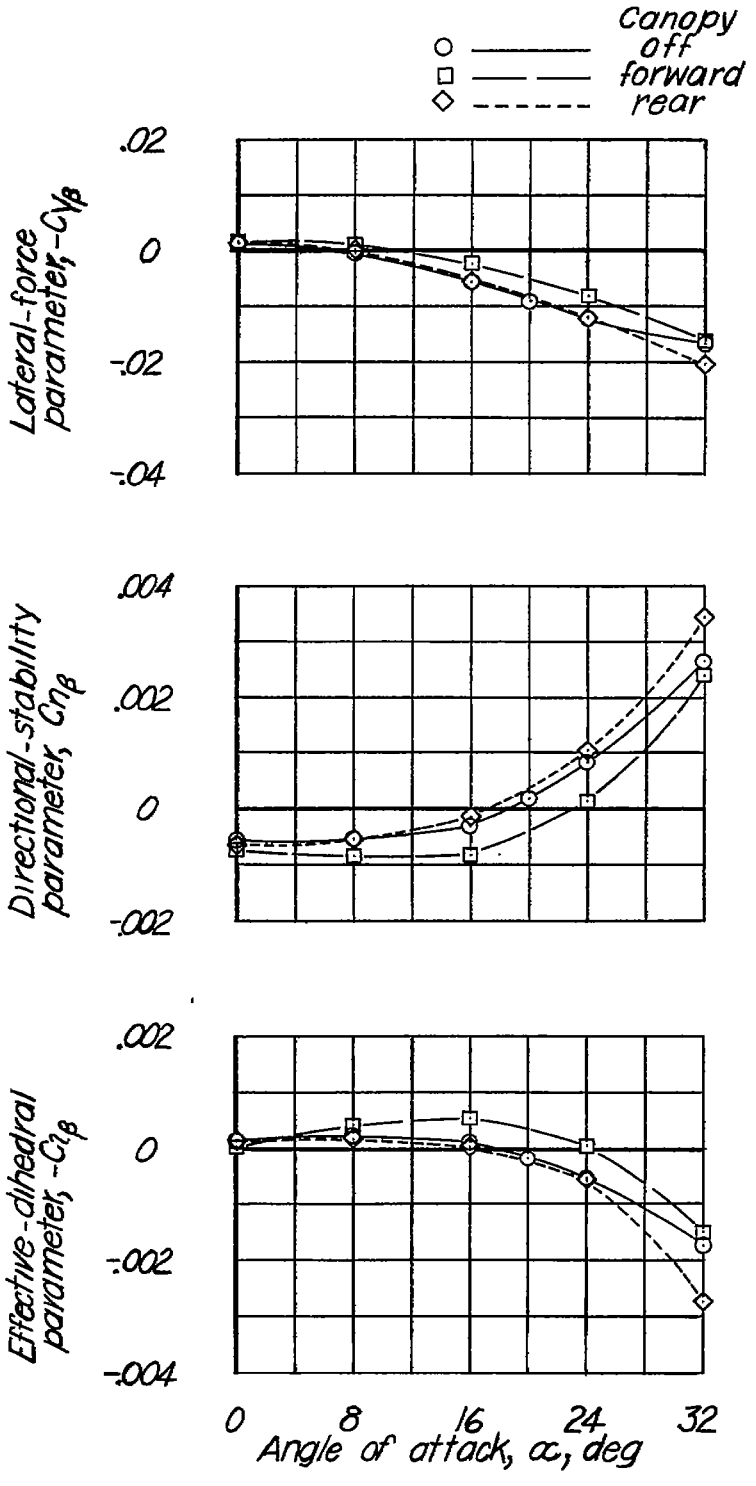

Figure 11.- Effect of canopy location on the lateral stability characteristics of model 4.

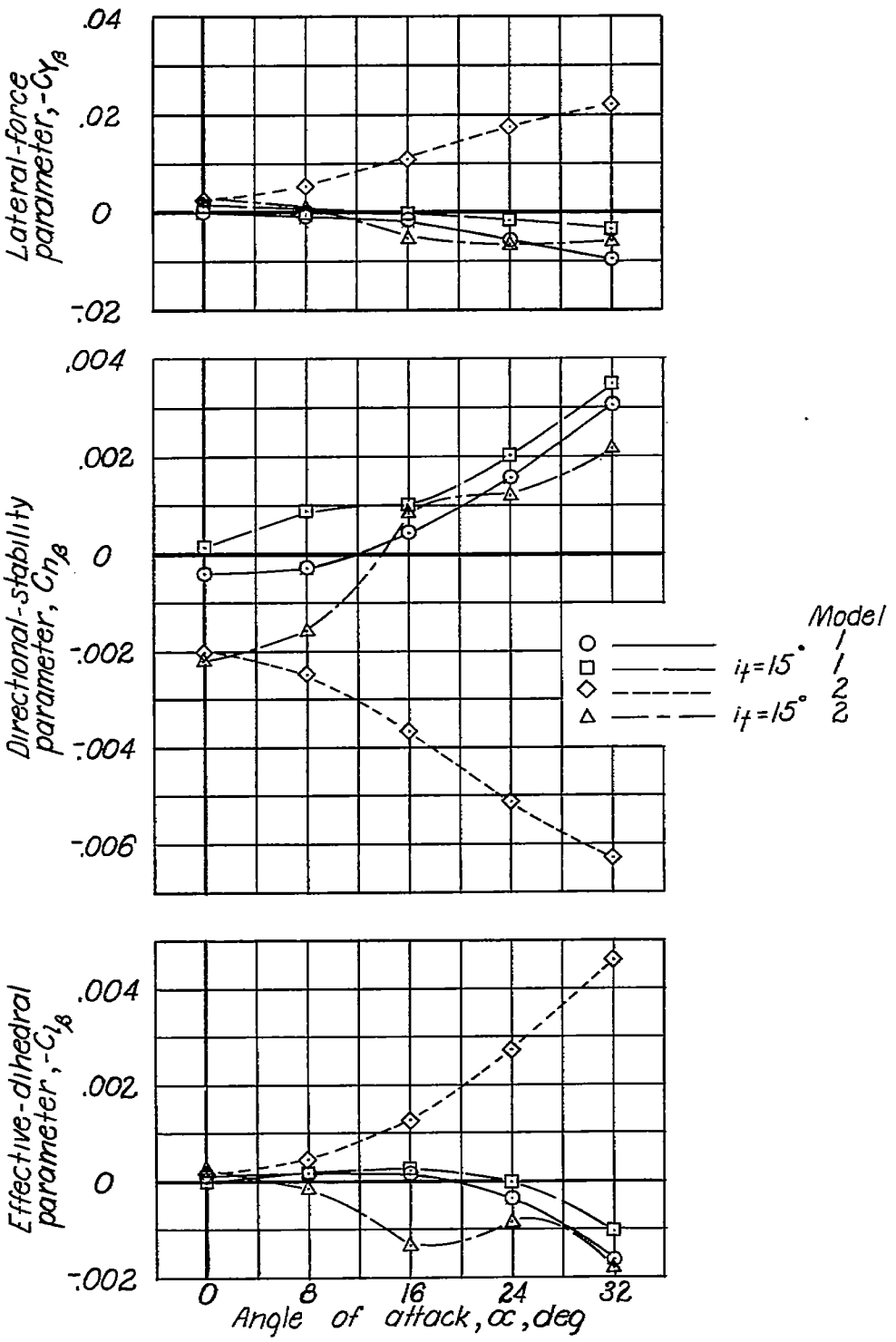

Figure 12.- Effect of a horizontal tail mounted at the nose (i_t = 15°) on the lateral stability characteristics of models 1 and 2.

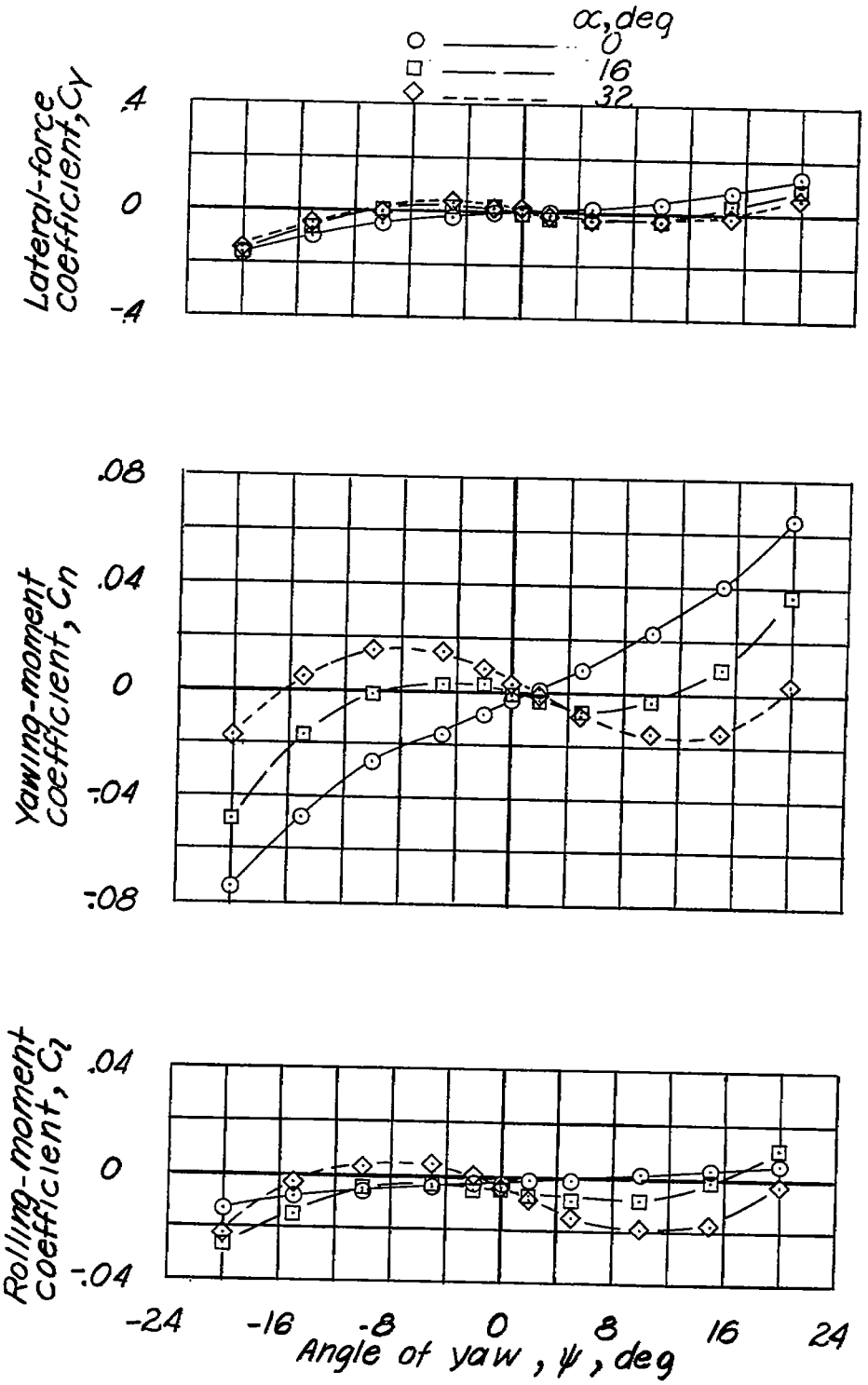

Figure 13.- Effect of angle of attack on the lateral-stability coefficients of model 2 with a horizontal tail.

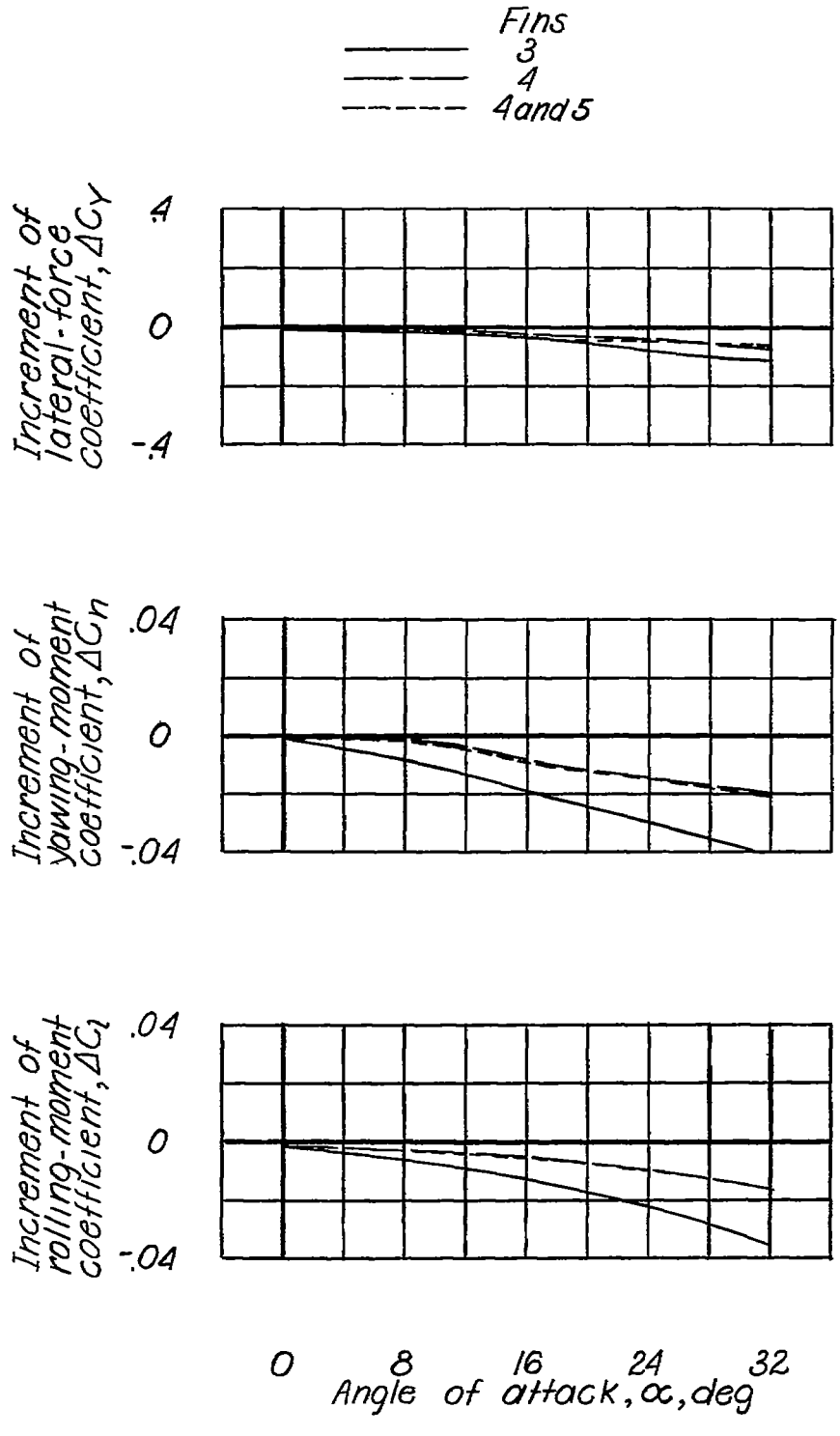

Figure 14.- Increments of lateral-stability coefficients caused by mounting asymmetric fins on model 1. $\Psi = 0^\circ$.

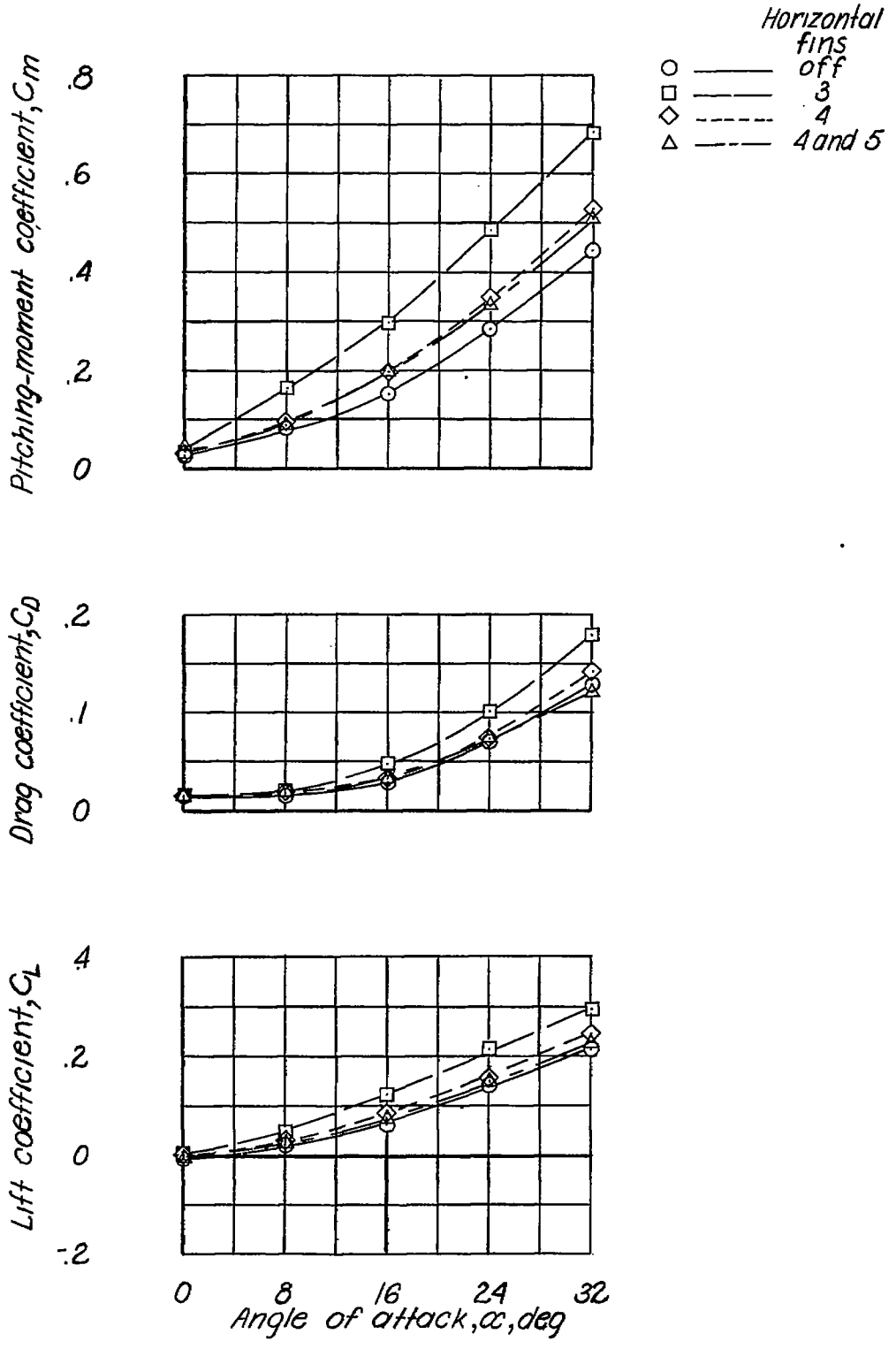

Figure 15.- Effect of horizontal fins on the longitudinal stability characteristics of model 1.

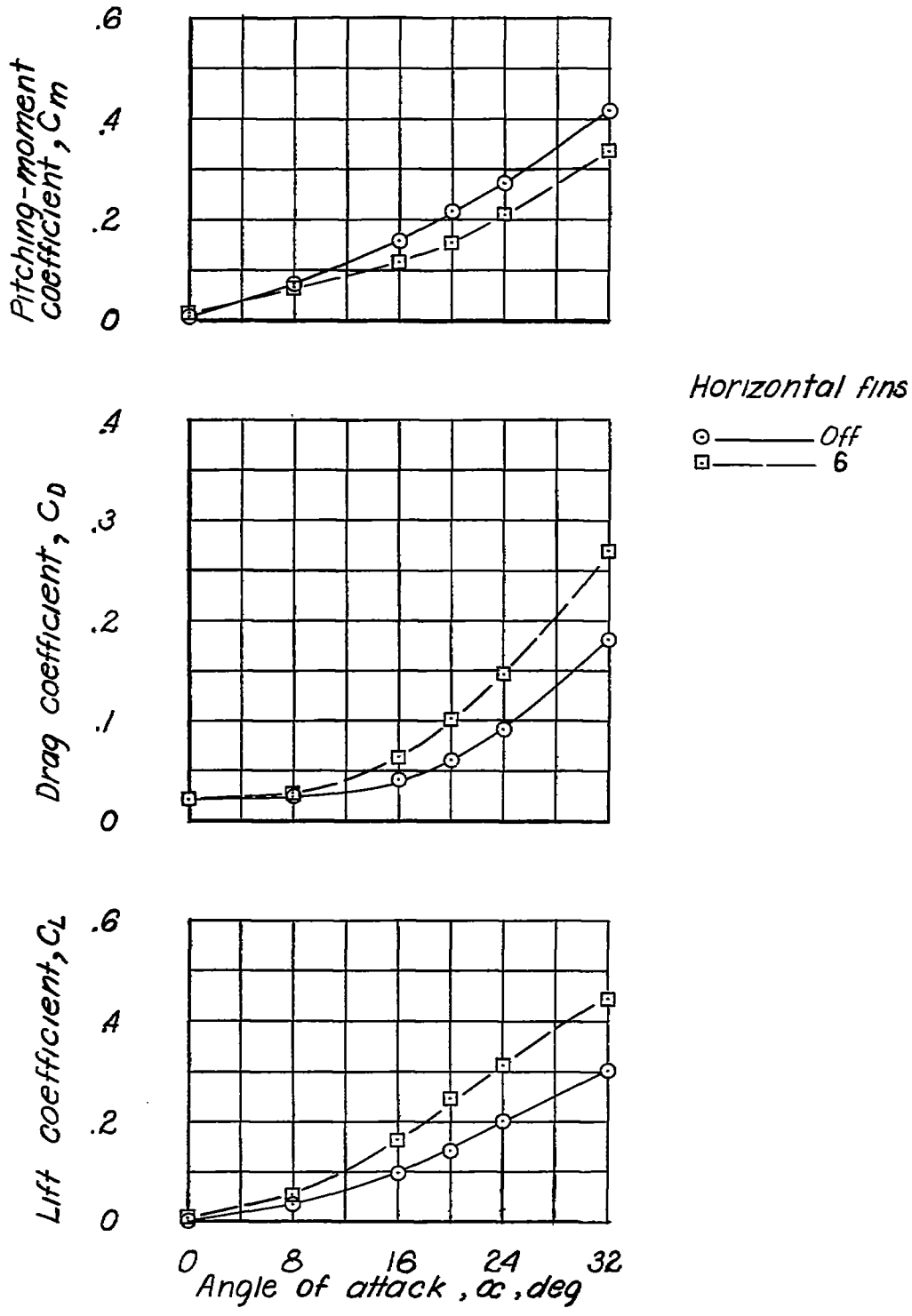

Figure 16.- Effect of horizontal fins on the longitudinal stability characteristics of model 4.